Improved Surface Chemistries, Thin Film Deposition Techniques, and Stamp Designs for Nanotransfer Printing

Etienne Menard,[†] Lise Bilhaut,[†] Jana Zaumseil,[‡] and John A. Rogers*[,†]

University of Illinois at Urbana/Champaign, Department of Materials Science and Engineering, Department of Chemistry, Beckman Institute and Seitz Materials Research Laboratory, Urbana, Illinois 61801, and Bell Laboratories, Lucent Technologies, Murray Hill, New Jersey 07974

Received May 11, 2004

Nanotransfer printing represents an additive approach for patterning thin layers of solid materials with nanometer resolution. The surface chemistries, thin film deposition techniques, and stamp designs are all important for the proper operation of this method. This paper presents some details concerning processing procedures and other considerations needed for patterning two- and three-dimensional nanostructures with low density of defects and minimal distortions.

Introduction

Lithographic techniques that use rubber stamps provide simple means to generate patterns with lateral dimensions that can be much smaller than 1 micron. These soft lithographic printing methods are useful for fabricating devices such as diodes,[1] photoluminescent porous silicon pixels,[2] organic light-emitting diodes,[3] thin-film transistors,[4] and a wide range of other devices in electronics and photonics, as well as biotechnology. The printed inks typically consist of soft organic materials such as proteins,[5] dendrimers, colloids, or molecules that form self-assembled monolayers.[6,7] Recent work demonstrates that similar stamps can print thin solid inks (i.e., polymer, metal, or inorganic films) of functional materials.[8,11−13] Such methods are purely additive in their operation. They do not suffer from loss of resolution due to etching steps or to surface spreading or vapor phase transport of the inks. One approach, referred to as nanotransfer printing, uses soft or hard stamps to print single or multiple layers of solid films.[8,14−16] It can form complex two- or three-dimensional[15] structures with minimum feature sizes well below 100 nm with edge resolution of 5−10 nm. The method has been used to build plastic[8] and molecular electronic devices[9,10] and subwavelength photonic elements.[16] This paper presents some improved surface chemistries, thin film deposition techniques, and advanced stamp designs for high-fidelity nanotransfer printing of metal films with elastomeric stamps made of poly(dimethylsiloxane) (PDMS). Some of these procedures are also important for a noninvasive electrical probing technique that uses thin metal films on PDMS elements.[17−19] The stamp designs are useful for a range of other soft lithographic methods.

Nanotransfer printing (nTP) relies on the transfer of a solid material ink from the structured surface of a stamp to a substrate. Figure 1 shows representative procedures for printing thin Au patterns. The process begins with deposition of the Au coating. In the case of Figure 1, a collimated flux of Au oriented perpendicular to the surface of a stamp forms a discontinuous coating on the raised and recessed regions. Contacting this stamp to a substrate that supports a self-assembled monolayer (SAM) designed to bond to the Au (e.g., a thiol-terminated SAM) leads to strong adhesion between the Au and the substrate. Removing the stamp, to which the Au only weakly adheres, transfers the Au on the raised regions of the stamp to the substrate. This purely additive printing approach offers exceptionally high resolution for two-dimensional patterning. With specially designed stamps, it is possible to transfer complex three-dimensional nanostructures. The printing steps can be repeated to build up patterned multilayer stacks.[15]

Results and Discussion

Surface Chemistry and Thin Film Deposition Effects on Nanotransfer Printing. The ability to

* Corresponding author. E-mail: jrogers@uiuc.edu.
† University of Illinois at Urbana/Champaign.
‡ Bell Laboratories.

(1) Goetting, L. B.; Deng, T.; Whitesides, G. M. *Langmuir* **1999**, *15*, 1182.
(2) Harada, Y.; Li, X.; Bohn, P. W.; Nuzzo, R. G. *J. Am. Chem. Soc.* **2001**, *123*, 8709.
(3) Koide, Y.; Wang, Q.; Cui, J.; Benson, D. D.; Marks, T. J. *J. Am. Chem. Soc.* **2000**, *122*, 11266.
(4) Kagan, C. R.; Breen, T. L.; Kosbar, L. L. *Appl. Phys. Lett.* **2001**, *79*, 3536.
(5) Bernard, A.; Delamarche, E.; Schmid, H.; Michel, B.; Bosshard, H. R.; Biebuyck, H. *Langmuir* **1998**, *14*, 2225.
(6) Kumar, A.; Whitesides, G. M. *Appl. Phys. Lett.* **1993**, *63*, 2002.
(7) Li, H.; Kang, D.-J.; Blamire, M. G.; Huck, W. T. S. *Nano Lett.* **2002**, *2*, 347.
(8) Loo, Y.-L.; Willett, R. L.; Baldwin, K. W.; Rogers, J. A. *Appl. Phys. Lett.* **2002**, *81*, 562.
(9) Hsu, J. W. P.; Loo, Y.-L.; Lang, D. V.; Rogers, J. A. *J. Vac. Sci. Technol., B* **2003**, *21*, 1928.
(10) Loo, Y.-L.; Lang, D. V.; Rogers, J. A.; Hsu, J. W. P. *Nano Lett.* **2003**, *3*, 913.
(11) Jiang, X.; Zheng, H.; Gourdin, S.; Hammond, P. T. *Langmuir* **2002**, *18*, 2607.
(12) Kim, C.; Shtein, M.; Forrest, S. R. *Appl. Phys. Lett.* **2002**, *80*, 4051.
(13) Loo, Y.-L.; Hsu, J. W. P.; Willett, R. L.; Baldwin, K. W.; West, K. W.; Rogers, J. A. *J. Vac. Sci. Technol., B* **2002**, *20*, 2853.
(14) Schmid, H.; Wolf, H.; Allenspach, R.; Riel, H.; Karg, S.; Michel, B.; Delamarche, E. *Adv. Funct. Mater.* **2003**, *13*, 145.
(15) Zaumseil, J.; Meitl, M. A.; Hsu, J. W. P.; Acharya, B. R.; Baldwin, K. W.; Loo, Y.-L.; Rogers, J. A. *Nano Lett.* **2003**, *3*, 1225.
(16) Loo, Y.-L.; Willett, R. L.; Baldwin, K. W.; Rogers, J. A. *J. Am. Chem. Soc.* **2002**, *124*, 7654.
(17) Zaumseil, J.; Someya, T.; Bao, Z.; Loo, Y.-L.; Cirelli, R.; Rogers, J. A. *Appl. Phys. Lett.* **2003**, *82*, 793.
(18) Loo, Y.-L.; Someya, T.; Baldwin, K. W.; Ho, P.; Bao, Z.; Dodabalapur, A.; Katz, H. E.; Rogers, J. A. *Proc. Natl. Acad. Sci. U.S.A.* **2002**, *99*, 10252.
(19) Lee, T.-W.; Zaumseil, J.; Bao, Z.; Hsu, J. W. P.; Rogers, J. A. *Proc. Natl. Acad. Sci. U.S.A.*, in press.

10.1021/la048827k CCC: $27.50 © 2004 American Chemical Society
Published on Web 07/03/2004

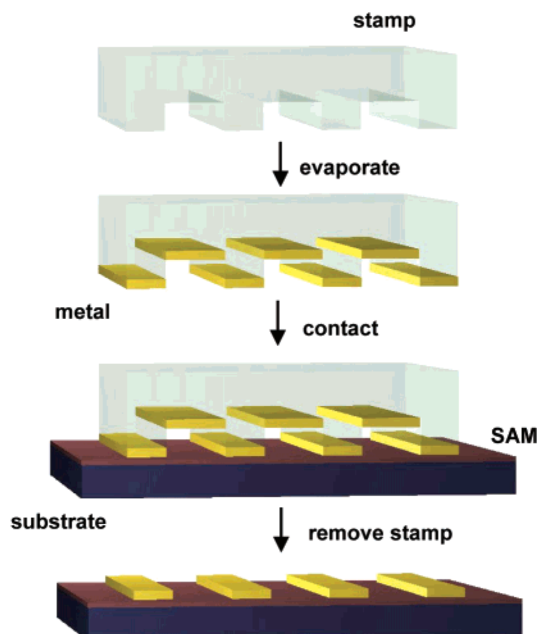

Figure 1. Schematic illustration of steps for nanotransfer printing. A collimated flux of material oriented perpendicular to the surface of a high-resolution stamp forms a discontinuous coating. (Au is illustrated here. Other materials are possible.) Contacting this coated stamp to a substrate leads to chemical reactions at the interface between the metal and the substrate. (A SAM provides the necessary chemistry.) These reactions bond the metal to the substrate; removing the stamp (to which the metal only weakly adheres) transfers the metal on the raised regions of the stamp to the substrate. Continuous coatings are also possible. In this case, the transfer process yields certain classes of three-dimensional structures.

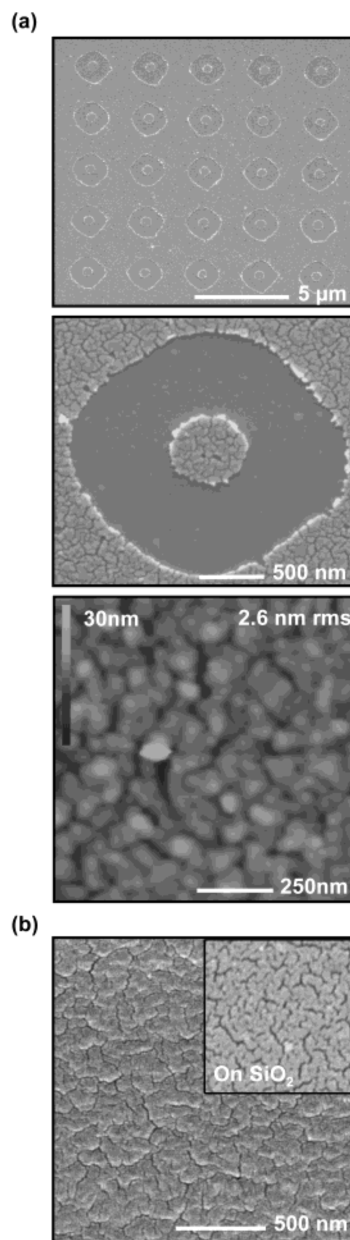

Figure 2. (a) Scanning electron micrographs (top two frames) and atomic force micrograph (third frame) of transfer-printed patterns of Ti/Au (2 nm/20 nm). (b) Scanning electron micrograph of a stamp coated with Ti/Au (2 nm/20 nm). SiO_2 wafer surface coated with Au (20 nm) in the inset.

perform nTP depends critically on processing conditions that enable robust coatings to be deposited on the stamps and to be transferred from them to substrates without damage. These challenges are significant when relatively brittle materials are printed with the types of elastomeric stamps that have been used in traditional soft lithography. Although nTP is compatible with rigid stamps, elastomeric ones are attractive because they are easy to fabricate and because they readily form intimate “wetting” contacts with a wide range of substrates without applied pressure. It is therefore important to develop processing conditions for using these types of stamps to fabricate defect-free patterns by nTP. The following focuses on printing of Au films onto either silicon wafers (with their native oxide) coated with a bilayer of Ti/Au (2 nm/20 nm) or onto GaAs wafers coated with a monolayer of octanedithiol. In the former case, cold welding between the freshly evaporated Au layers on the stamp and substrate guides the transfer of the metal patterns.[12,16] In the latter case, Au−S bonds facilitate transfer.[13] In both systems, contact between the stamp and substrate for a few seconds is sufficient to induce bonding. *The coating and deposition conditions are chosen to ensure that the strength of adhesion between the metals and the stamps is small compared to the adhesive bonds that form to the substrate during contact.*

The stamps use bilayer PDMS designs described elsewhere.[20] These stamps are placed on glass slides immediately before depositing the Au; they remain on these slides throughout the course of the printing process. Rigid backings help to eliminate damage to the coatings that can otherwise be introduced during manipulation of the stamps. Electron beam evaporation of thin Au (20 nm) onto the stamps at relatively high rates (1 nm/s) yields smooth, electrically continuous coatings that are free of the rippling observed in other work.[21] Figure 2a shows field-emission scanning electron micrographs (SEMs) and atomic force micrographs (AFMs) of typical patterns that result from nTP by cold welding onto a silicon substrate (similar results are obtained with the GaAs system). Although printing in this manner successfully forms high-resolution patterns over large areas, Figure 2a shows that nanoscale cracking in the Au can occur. Imaging of coated stamps before printing (Figure 2b) indicates that the nanocracking is already present at that stage of the process. Contacting and removing the stamp from the substrate, when carried out carefully with stamps mounted

(20) Odom, T. W.; Love, J. C.; Wolfe, D. B.; Paul, K. E.; Whitesides, G. M. *Langmuir* **2002**, *18*, 5318.

(21) Bowden, N.; Brittain, S.; Evans, A. G.; Hutchinson, J. W.; Whitesides, G. M. *Nature* **1998**, *393*, 146.

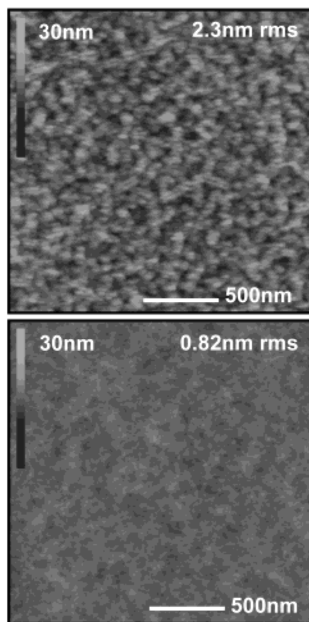

Figure 3. Atomic force micrographs of an evaporated Ti/Au metal layer on the surface of PDMS/gelest stamps. The top frame corresponds to Ti/Au (2 nm/20 nm) deposited directly onto the untreated surface of the stamp. The second frame illustrates results obtained when the stamp is exposed to a short (13 s) oxygen plasma treatment before deposition of the metals. Crack-free patterns of smooth (root-mean-square roughness of <1 nm) gold films can be obtained in this manner.

on glass slides for support, does not seem to alter significantly the density or length scale of these cracks. This type of defect is often present when only Au is used; it is somewhat less frequently observed when Ti (1−2 nm) is used as an interfacial wetting layer between the Au and PDMS. The morphology and density of these nanocracks seem to be only weakly related to the physical properties (modulus, thermal expansion coefficient, etc.) of the PDMS stamps. (We noticed that evaporated Au films on in situ heated PDMS stamps present identical film structure with a similar density of nanocracks.) In fact, similar nanocracking is present in 20 nm Au coatings deposited in the same manner onto bare silicon wafers with their native oxide (Figure 2b inset). In this case, a thin adhesion-promoting layer of Ti (1−2 nm) deposited before the Au eliminates the cracks. *Collectively, these observations suggest that it is the composition and deposition conditions for the metal layers that primarily control the presence of cracks, rather than the physical properties of the stamps, the methods for printing, or the transfer bonding of the metals.* We exploit this fact for nTP by first exposing PDMS to an oxygen plasma to create a silica-like surface layer[22,23] and then depositing Ti (2 nm at 0.3 nm/s) and Au (20 nm at 1 nm/s). These procedures yield smooth metal coatings that are free of cracks. See Figures 3 and 4b. The time and conditions of the plasma treatment and the thickness of the Ti control the degree of adhesion of these coatings to the PDMS (i.e., reducing the oxygen plasma or thickness of Ti reduces the adhesion). Strong adhesion is useful for applications in soft contact lamination, where the coatings remain on the PDMS in the final device geometry. For nTP, the adhesion should be as weak as possible to facilitate transfer. Sufficiently poor adhesion

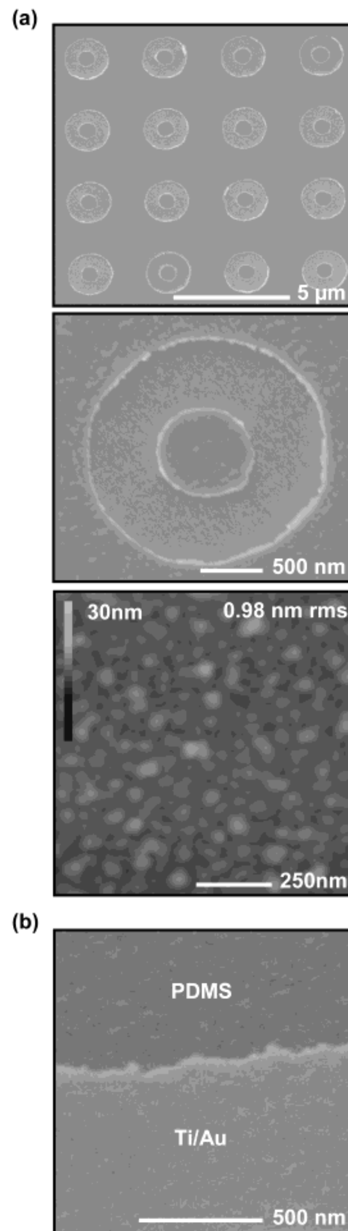

Figure 4. (a) Scanning electron micrographs (top two frames) and atomic force microscope image (third frame) of a pattern printed with optimized conditions. (b) Scanning electron micrographs of the surface of a stamp coated with Ti/Au (2 nm/20 nm). The results indicate that nanotransfer printing can reliably form Au patterns that are smooth and crack free (as observed with atomic force microscopy and scanning electron microscopy).

of coatings that are free of nanocracks can be obtained by minimizing the duration of the oxidation step and the thickness of the Ti layer. Figure 4a shows the results.

X-ray photoelectron spectroscopy (XPS) indicates that patterns printed in this manner are often coated with an ultrathin layer of PDMS-like material. We speculate that this layer improves the physical toughness of the printed films, thereby aiding in the formation of defect-free patterns. Its thickness and extent of coverage are sensitive functions of the processing conditions. Figure 5 summarizes XPS measurements on transferred patterns of Ti/Au before and after exposure to a brief reactive ion etch (RIE) (60 s using an Uniaxis 790 Plasma-Therm reactive ion etching system in an oxygen flow of 10 standard cubic centimeters per minute (sccm) and 30 sccm

(22) Jeon, N. L.; Clem, P. G.; Nuzzo, R. G.; Payne, D. A. *J. Mater. Res.* **1995**, *10*, 2996.
(23) Duffy, D. C.; McDonald, J. C.; Schueller, O. J. A.; Whitesides, G. M. *Anal. Chem.* **1998**, *70*, 4978.

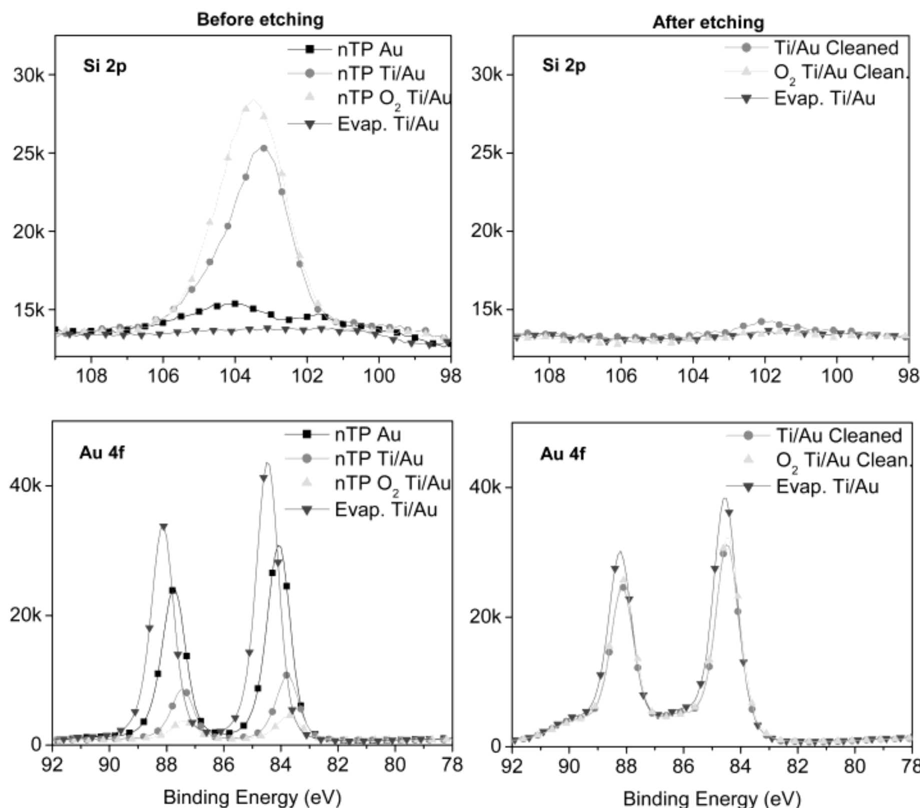

Figure 5. X-ray photoelectron spectroscopy of nanotransfer-printed patterns of Ti/Au. The data were collected before (left side spectra) and after (right side spectra) treatment of the patterns with a reactive ion etch to remove residual organics from the surfaces of the printed films. The results show that these organics, which originate from the poly(dimethylsiloxane) stamps and are present as ultrathin films (~2 nm thick, depending on processing conditions), can be removed effectively by dry etching. The intensities of the Au and Si peaks confirm that the cleanness of the RIE-cleaned gold patterns is comparable to that of freshly evaporated Ti/Au film onto a bare silicon wafer (here included for comparison purposes).

of CF_4 at a chamber pressure of 30 mTorr with a 50 W radio frequency (rf) power). The disappearance of the Si-(2p) peak and intensity increase of the Au(4f) peaks indicate that these coatings can be removed by this type of etching. Similar results are obtained with wet etching (5 min of immersion in a boiling hydrogen peroxide solution). Figure 6a shows AFM images of transferred coatings before and after exposure to the RIE. *The etching induces little or no change in the morphology of the film.* AFM analysis of a step edge (Figure 6b) caused by RIE etching through a mask indicates that these coatings are approximately 2 nm thick (with a 1 or 2 nm variation depending on the conditions for the plasma oxidation step). *XPS experiments indicate that some Ti transfers to the substrate. If needed, this ultrathin layer can be briefly etched away in a HF/H_2O 1:10 solution which does not damage the Au film.*

Two- and Three-Dimensional Printing Using Optimized Stamp Relief Profiles. Three-dimensional nanostructures result from nanotransfer printing of ink coatings deposited not only on the raised and recessed regions of the stamps but also on their sidewalls. Figure 7 shows SEMs of some representative structures formed in this manner using the processing approaches described in the previous section. The top frames show an array of sealed nanocapsules formed by printing a continuous, conformal coating of Ti/Au (1.5 nm/15 nm) on a stamp that has an array of holes (i.e., arrays of cylindrical depressions, 500 nm diameters and 300 nm deep) on its surface. Using a stamp with the inverse geometry (i.e., arrays of posts) produces the crossed nanochannel system shown in the middle frames. Structures with an “L” geometry result from printing with a stamp that has surface relief in the geometry of an array of lines and is coated using a steeply angled flux of metal. The mechanical integrity of these features is remarkable. The ability to print structures of this sort depends critically on processing conditions that enable robust crack-free coatings to be formed and transferred.

For the three-dimensional structures of Figure 7, sloping sidewalls on the stamp help to enable continuous ink coatings. To print two-dimensional patterns with sharp, well-defined edges, vertical or re-entrant sidewalls must be used with a deposition flux collimated normal to the surface of the stamp. The sensitivity of printed two-dimensional patterns to stamp geometry and deposition conditions can be reduced by incorporating sharply re-entrant features of relief near the contact surface of the stamp. Figure 8a schematically illustrates this approach. Fabrication of the necessary stamps begins by spin coating a silicon wafer with a layer of liftoff resist followed by conventional positive photoresist. Exposing and developing this bilayer resist removes selectively the positive resist in the areas that are exposed. The same developer also removes exposed or unexposed liftoff resist. The resulting structure consists of a pattern of the positive resist in the geometry of the photomask. By proper selection of development conditions, the liftoff resist can be removed completely in the exposed regions and to a small extent in the unexposed regions underneath the remaining positive resist. The latter effect yields a small undercut at the edges of the positive resist. For the experiments described here, the thickness of the liftoff resist was ~100 nm and the degree of undercut was ~100 nm. Casting and curing PDMS against this type of master in the usual way generates stamps with T-shaped tops. The elastomeric

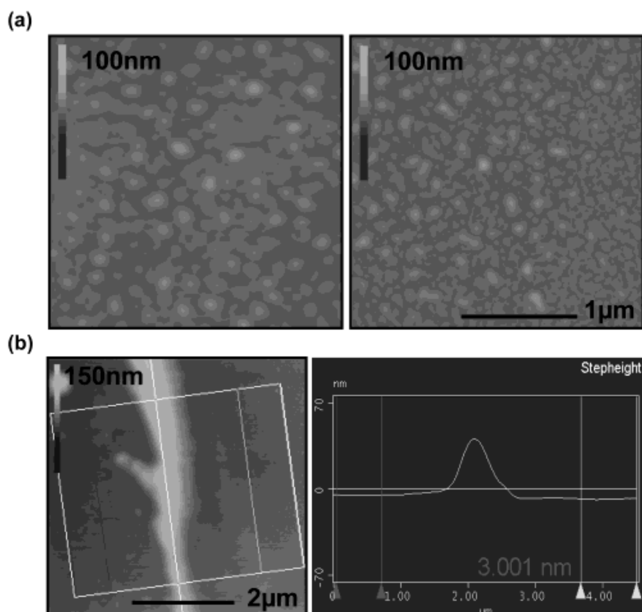

Figure 6. (a) Atomic force micrographs of patterns of Au/Ti formed by nanotransfer printing with optimized procedures. The images show representative areas of patterns before and after exposure to a reactive ion etching step that removes residual organics from the surfaces of the metal films. (b) Atomic force micrograph and cross-section analysis of a transferred silica-like coating etched by RIE through a membrane; the thickness of the residual organic layer is measured to be ~3 nm (×b11 nm). The line cut represents the average of many line scans collected across the step.

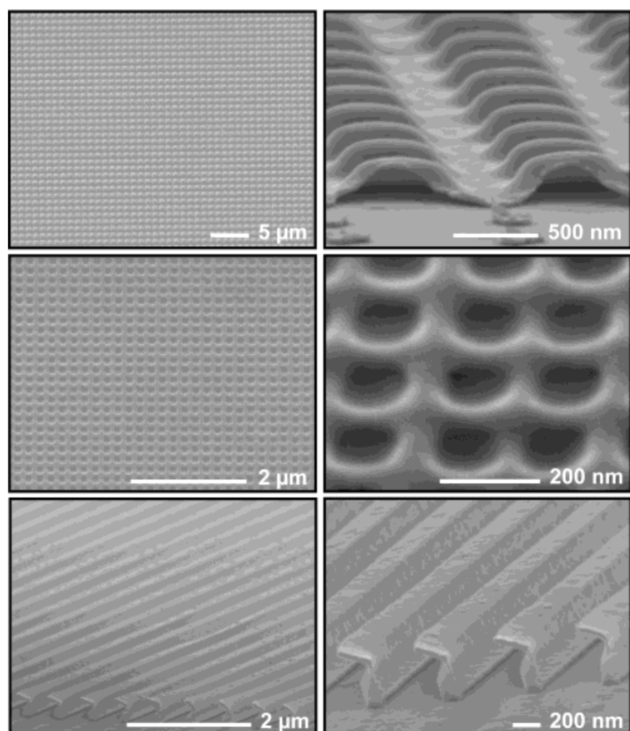

Figure 7. Scanning electron micrographs of representative three-dimensional structures formed by nanotransfer printing. The left and right images show low- and high-magnification views, respectively. The top frames show arrays of sealed nanocapsules; the middle frames show a square grid of crossed nanochannels; the bottom frames show free-standing L-shaped beams.

nature of the PDMS enables stamps with these geometries to release nondestructively from the master. Figure 8b

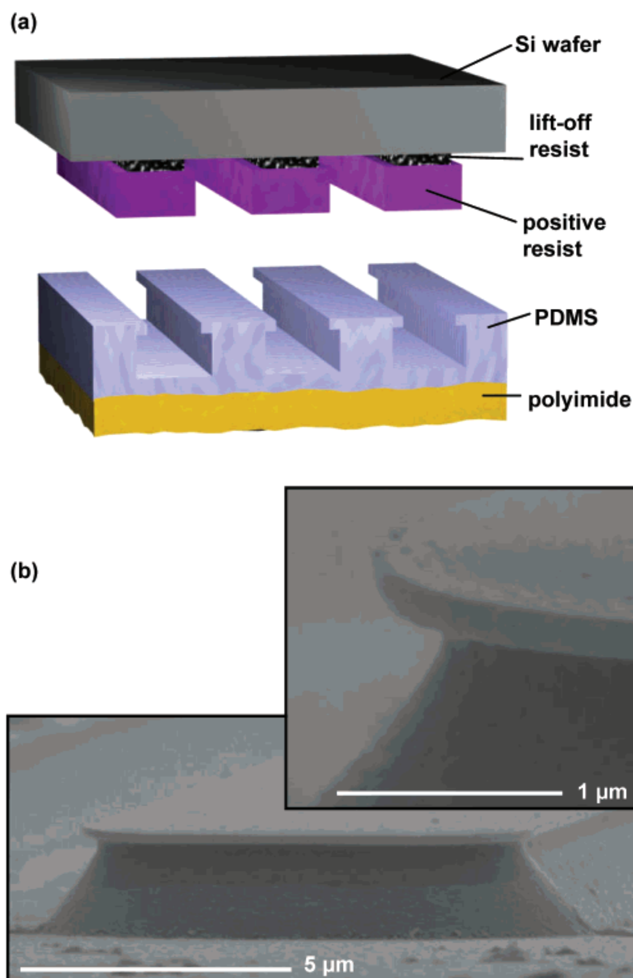

Figure 8. Schematic illustration (part a) of re-entrant stamps designed for high-fidelity, two-dimensional nanotransfer printing. A pattern of photoresist with an underlying layer of liftoff resist forms a master for generating PDMS stamps that have re-entrant profiles. Such designs prevent the deposition of metal onto the relief sidewalls near the top surfaces of the stamps, even when these sidewalls are steeply sloped. The scanning electron micrograph in part b illustrates this effect; it shows a re-entrant stamp with a thin layer of Au evaporated using a collimated flux oriented perpendicular to the surface of the stamp. A shadowed area that is free of Au is visible underneath the protruding re-entrant feature of the stamp.

shows an SEM image of the relief structure on a typical stamp that has been coated with Au. A shadowed region beneath the overhang at the top of the stamp is visible. Figure 9 presents an AFM image of an edge region of a pattern produced by nTP with a stamp of this type. It also shows an image of a similar pattern generated with a stamp that has the same sidewall geometry, but without the sharply re-entrant structure associated with the liftoff resist. These results illustrate that the optimized stamp design eliminates the raised region at the edge of the Au feature printed with the conventional stamp. The liftoff masters and associated stamps could be used multiple times without damage.

Tough, Flexible Stamps That Use Thin Polymer Backings. As we have described previously, placing thin elastomeric stamps against glass slides enhances their structural rigidity, thereby minimizing in-plane deformations that can lead to cracks in the solid inks during manipulation of the stamps before and during printing. This stamp design also reduces distortions that can frustrate accurate multilevel registration.[24] A disadvan-

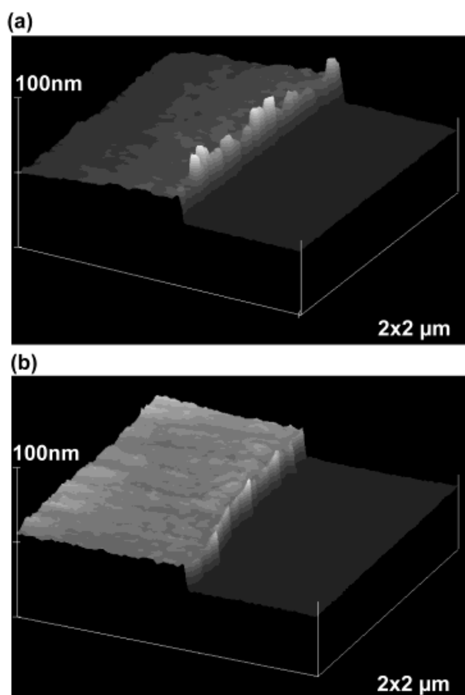

Figure 9. Atomic force microscope images of the edges of nanotransfer-printed patterns of Au/Ti on GaAs. The edges in the patterns defined with unoptimized stamps (top) are rougher and have greater relief than those generated with re-entrant stamps (bottom). The improved edges in the latter case derive mainly from the ability of the re-entrant structure to prevent deposition of Au/Ti on the top parts of the sidewalls of the sloping relief features on the normal stamp.

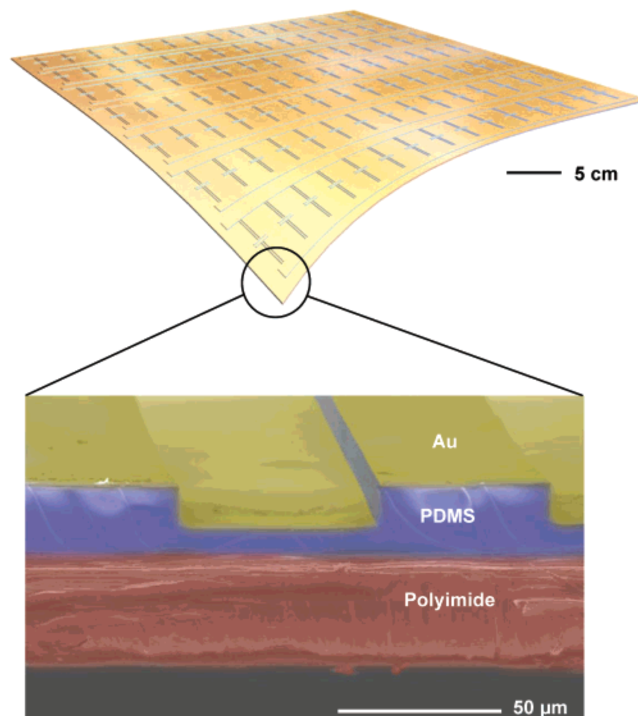

Figure 10. Schematic illustration (top) and cross-sectional scanning electron micrograph (bottom) of a composite stamp. The structure consists of a thin layer of poly(dimethylsiloxane) bonded to a thin layer of polyimide. The resulting stamp is mechanically robust and flexible, and it is easy to use for printing. It has a relatively high in-plane modulus (5.3 GPa, defined mainly by the polyimide) that helps to reduce distortions that can occur in printing. The polyimide backing layer also decreases the tendency of the stamp to make unwanted contact with the substrate due to mechanical sagging in its recessed regions.

tage is that the thick glass backings make it difficult to bend the stamps. Bendability is important because it allows stamp−substrate contact to be established in a gradual, controlled manner that avoids trapped air pockets.[25] It also enables easy separation, by peeling, of stamps from their master or from a substrate. Although thin glass backing layers enable bending, they can be mechanically fragile and require the application of a uniform pressure on their backing for printing on uneven substrates.[26] Replacing the glass sheets with thin films of polymers that have a relatively high modulus yields composite stamps that (i) are easy to use for printing, molding, and other soft lithographic techniques, (ii) avoid in-plane deformations that can damage solid ink coatings for nanotransfer printing, and (iii) lead to pattern distortions that are sufficiently low for micron-level pattern registration over large areas. To demonstrate this concept, we built large-area composite stamps using thin (5−10 μm) PDMS layers with sheets of polyimide (Kapton E, 25 μm thick, DuPont) as backing layers. We typically also included with these stamps a thick (∼10 mm) PDMS flat or a second polyimide film separated by another thin (∼4 μm) PDMS layer, to facilitate handling and to avoid the curling that can occur after separation from the master (due to shrinkage of the PDMS and/or mismatch in the thermal expansion coefficients of the PDMS and the polyimide). Figure 10 shows a schematic illustration and a cross-sectional SEM. For this example, the relief layout corresponds to the source/drain level of an active matrix circuit for electronic paper displays. It consists of 256 interconnected transistors arranged in a square array over an area of 16 × 16 cm.[27] We quantified the distortions in these composite stamps by measuring with a microscope the misalignment at each transistor location between two successive prints, between one print and the stamp used to print and between a stamp and its master. Figure 11 shows distortions that correspond to measurements of positions of features on the stamp compared to those on its master. These results include corrections for overall translational and rotational misalignment and isotropic shrinkage (280 ppm for stamps cured at 80 °C and 60 ppm for those cured at room temperature). The residual distortions are close to the estimated accuracy (∼1 μm) of our measurement method. They include the cumulative effects of (i) fabricating and releasing the stamp from its master and (ii) printing (wetting the stamp) on an uneven substrate (the master has some relief features ∼9 μm thick).

Another attractive feature of the composite stamps is that they have a reduced tendency to sag mechanically in the recessed regions, which can cause unwanted stamp−substrate contact.[28] As an example, in the case of 60 μm wide lines separated by 60 μm (500 nm relief height), recessed areas of a regular single element PDMS stamp sag completely. No sagging is observed for the same relief geometry on a PDMS/polyimide/PDMS/polyimide (25/25/60/25μm) composite stamp. Figure 12 shows top view

(24) Folch, A.; Schmidt, M. A. *J. Microelectromech. Syst.* **1999**, *8*, 95.
(25) Burgin, T.; Choong, V.-E.; Maracas, G. *Langmuir* **2000**, *16*, 5371.
(26) Michel, B.; Bernard, A.; Bietsch, A.; Delamarche, E.; Geissler, M.; Juncker, D.; Kind, H.; Renault, J. P.; Rothuizen, H.; Schmid, H.; Schmid-Winkel, P.; Stutz, R.; Wolf, H. *IBM J. Res. Dev.*. **2001**, *45*, 706.
(27) Rogers, J. A.; Paul, K. E.; Whitesides, G. W. *J. Vac. Sci. Technol., B* **1998**, *16*, 88.
(28) James, C. D.; Davis, R. C.; Kam, L.; Craighead, H. G.; Isaacson, M.; Turner, J. N.; Shain, W. *Langmuir* **1998**, *14*, 742.

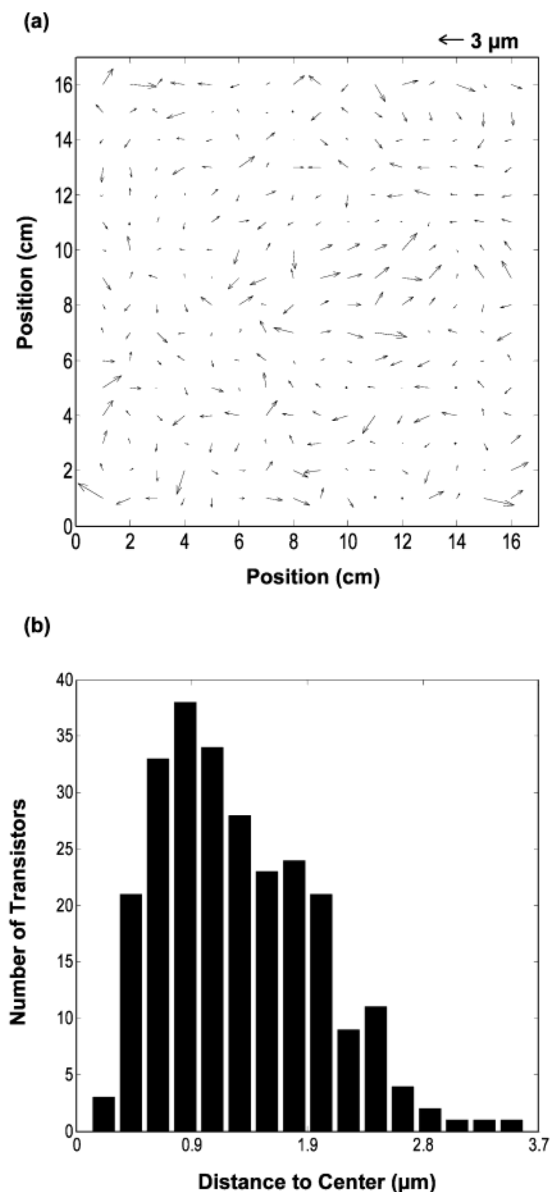

Figure 11. Distortion measurements collected at 256 points equally spaced across a 16 × 16 cm stamp that has the layout of the source/drain level of an active matrix backplane circuit for an electronic paper display. The top frame shows a vector diagram of misalignments between the stamp (which uses a composite design) and its master. (Overall translational and rotational misalignments are subtracted.) The bottom frame shows a histogram plot of the lengths of the vectors illustrated in the top frame. The median distortion is less than 1 micron. This value is better, by ~25 times, than results observed by us with conventional single-component stamps of poly(dimethylsiloxane) that have the same layout.

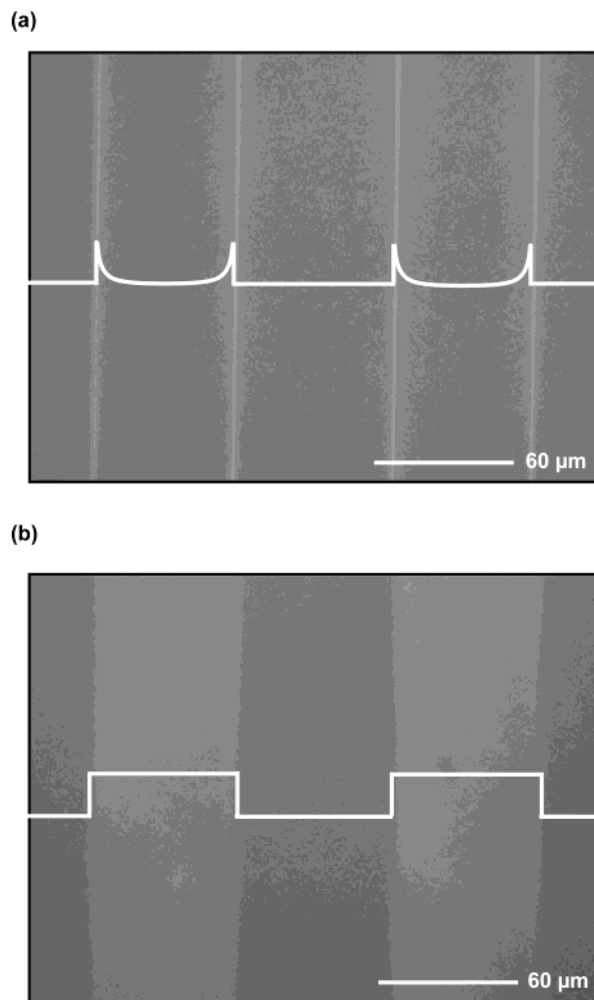

Figure 12. Optical micrographs (parts a and b) of stamps placed against glass slides, obtained by imaging through the stamps. The lines schematically illustrate the shape of the relief (500 nm height) on the stamp after contact. Part a indicates complete sagging of the recessed regions of a conventional single-component PDMS stamp. Part b shows a similar image of a composite stamp that uses the same PDMS chemistry, but in a thin film (~25 μm) geometry supported by a thin (25 μm) polyimide sheet. This stamp shows no evidence of sagging.

optical micrographs that illustrate these results. The color uniformity in the recessed area of the composite stamp (Figure 12b) suggests that the bowing is almost zero. Finite element modeling of the composite structure indicates that the Kapton backing efficiently reduces the tendency of the stamp for sagging when the residual PDMS layer is thin. These simulations results will be presented in a different publication.

Conclusions

The surface chemistries, thin film deposition techniques, and stamp designs presented in this paper enable patterning, with high fidelity and low defect density, of two- and three-dimensional nanostructures by nanotransfer printing. The successful fabrication of self-supporting discontinuous three-dimensional metal nanostructures, in particular, demonstrates the efficiency of some of these procedures. The morphology of the transferred patterns is, however, highly sensitive to the preparation of the stamp surface prior to metallization. For example, in some cases the plasma oxidation treatment can form low-density shallow (10 nm deep), small diameter (30 nm) depressions on the surface of the stamp. This effect leads to small gold bumps on the surface of the transferred film. See Figure 6a. In other cases, excessive plasma treatment leads to a failure interface upon transfer that is cohesive at a depth of some microns below the surface of the stamp. Careful process control can eliminate these effects. It is likely that similar optimization through study of surface chemistry will be required for printing of materials other than those explicitly described here. The low level of distortions observed in easy-to-use, flexible composite stamp designs indicates that the printing method, in its current form, can meet the requirements of applications in plastic electronics and in many areas of subwavelength and integrated optics. These features suggest that nTP may

represent a versatile tool for patterning, in a purely additive fashion, materials with nanometer resolution.

Experimental Section

Printing Procedures. Metal evaporation was performed with a Temescal electron beam system (BJD 1800) and deposition rates of 0.3 nm/s for Ti and 1 nm/s for Au. Pressures during evaporation were typically $\sim 3 \times 10^{-6}$ Torr or less. A deposition rate monitor was installed in position such that the rates could be established and stabilized before exposing the stamps or substrates to the flux of metal. The printing was performed in open air shortly after deposition. The stamps typically come into intimate contact with the substrates without applied pressure. In some cases, small pressure applied by hand initiated contact at one edge, which then proceeded naturally across the stamp–substrate interface. Peeling the stamp away from the substrate after contact for a few seconds completed the printing. The stamps used either glass slides or thin sheets of polyimide as structural supports to prevent unwanted in-plane strains during processing or printing.

Fabrication of Stamps with Re-entrant Sidewalls. Masters with sharply re-entrant profiles used positive photoresist (S1818; Shipley, www.shipley.com) and liftoff resist (LOR1A; MicroChem, www.microchem.com). Test grade ~ 450 μm thick silicon wafers (Montco Silicon Technologies, www.silicon-wafers.com) were cleaned with acetone, 2-propanol, and deionized water and then dried on a hotplate at 150 °C for 10 min. In the first step, LOR1A resin was spin-coated at 3000 rpm for 30 s and then prebaked on a hot plate at 130 °C for 5 min. Next, the S1818 resin was spin-coated at 3000 rpm for 30 s and baked on a hot plate at 110 °C for 5 min. The resulting bilayer film (~ 1.7 μm thick) was exposed ($\lambda = 365$ nm, 16.5 mW/cm^2 for 7 s) with an optical contact aligner (Suss Microtech MJB3) using a chromium on glass mask and then developed (MF-319; Shipley) for 75 s. This development removed all of the S1818 resist that was photoexposed. It also removes, in a roughly isotropic manner, the LOR1A in both the exposed and unexposed regions. The result is a pattern of S1818 on LOR1A with regions of bare substrate in the exposed areas and slight undercuts at the edges of the patterns. Standard soft lithographic procedures of casting and curing PDMS against these patterns produce stamps with the desired sharply re-entrant features.

Fabrication of Stamps with Flexible Polymer Backings. Masters were prepared with conventional contact mode photolithography (features larger than 2 μm) or electron beam lithography (features smaller than 2 μm). The masters for the large-area stamps were formed by direct write photolithography using procedures described elsewhere.[29] PDMS (Sylgard 184 from Dow Corning, www.downcorning.com) or h-PDMS (VDT-731, Gelest Corp., www.gelest.com) was mixed and degassed, poured over the masters, and cured in a oven at 80 °C. In some cases, the curing of the 184 PDMS material was performed at room temperature, by using twice as much curing agent as recommended by the vendor of this material. Kapton polyimide films 100E (DuPont, www.dupont.com/kapton) were plasma-oxidized using an Uniaxis 790 Plasma-Therm reactive ion etching system in an oxygen flow of 20 sccm at a pressure of 30 mTorr for 3–5 min with a 100 W rf power. A few drops of h-PDMS were dispensed onto the surface of the master, and then the Kapton sheet was slightly bent and brought into contact with the master (plasma-treated side facing down). Air bubble formation was prevented by slowly bringing down the full sheet of plastic from the center toward the edges. Rolling a glass cylinder over the surface of the sheet reduced the thickness of the PDMS layer to 5–10 μm.

Instrumentation. AFM images were recorded using a Dimension 3100 microscope in tapping mode. The images were analyzed using the Nanoscope IV v5.12b18 software package (Digital Instruments, Santa Barbara, CA). SEM images were recorded using a Philips XL30 field-emission environmental scanning electron microscope (ESEM-FEG) in high-vacuum mode. All images were recorded with an accelerating voltage of 5 keV and a gun–sample distance of 10 mm. XPS spectra were obtained using a Kratos Axis Ultra photoelectron spectrometer using Al KR radiation (15 kV, 225 W, base pressure $\sim 5 \times 10^{-10}$ Torr). High-resolution spectra of the Si(2p) and Au(4f) core levels were collected at a pass energy of 40 eV with a 1.0 mm^2 spot size. The binding energies were normalized and corrected by referencing the C(1s) binding energy to 284.5 eV. High-resolution spectra backgrounds were corrected using a linear fitting function for the baseline.

Acknowledgment. The authors thank Rick Haasch for technical support and helpful discussions regarding the XPS analysis. XPS acquisition and AFM imaging were carried out in the Center for Microanalysis of Materials, University of Illinois, which is partially supported by the U.S. Department of Energy under Grant DEFG02-91-ER45439. SEM imaging was carried out using the equipment of the Imaging Technology Group of the Beckman Institute for Advanced Science and Technology.

LA048827K

(29) Rogers, J. A.; Bao, Z.; Baldwin, K.; Dodabalapur, A.; Crone, B.; Raju, V. R.; Kuck, V.; Katz, H.; Amundson, K.; Edwing, J.; Drzaic, P. *Proc. Natl. Acad. Sci. U.S.A.* **2001**, *98*, 4835.